Eur. Phys. J. C 11, 89–92 (1999)
Digital Object Identifier (DOI) 10.1007/s100529900173

THE EUROPEAN PHYSICAL JOURNAL C

Non-singlet corrections of $\mathcal{O}(\alpha_s^2 G_F M_t^2)$ to $\Gamma(Z \to b\bar{b})^\star$

K.G. Chetyrkin[1,a], M. Steinhauser[2]

[1] Institut für Theoretische Teilchenphysik, Universität Karlsruhe, D-76128 Karlsruhe, Germany
[2] Institut für Theoretische Physik, Universität Bern, CH-3012 Bern, Switzerland

Received: 16 March 1999 / Published online: 3 August 1999

Abstract. The partial decay rate of the Z boson into bottom quarks constitutes an important decay channel. This is mainly due to the virtual presence of the top quark in the loop diagrams giving rise to correction factors which are quadratic in the top quark mass. At one- and two-loop order it turned out that the leading term in the heavy-top expansion leads to very good approximations to the exact result. In this work the non-singlet diagrams at $\mathcal{O}(\alpha_s^2 G_F M_t^2)$ are considered.

The impressive experimental precision mainly at the Large Electron Positron collider (LEP) at CERN, the Stanford Linear Collider (SLC) and the FERMILAB Tevatron in Chicago has made it mandatory to evaluate higher order quantum corrections to the processes observed in the experiments [1]. The strategy to combine experimental information with theoretical computations has successfully been applied to the search for the top quark several years ago. Nowadays the same concept is used in order to pin down the mass of the Higgs boson, the only not yet discovered particle of the Standard Model of elementary particle physics.

An important observable is the decay of the Z boson into bottom. QCD corrections are known up to $\mathcal{O}(\alpha_s^3)$ (for a comprehensive review see [2]). The electroweak one-loop corrections are known since quite some time [3]. They have the interesting feature that the top quark appears virtually in the loop diagrams. Recently also the full corrections of $\mathcal{O}(\alpha\alpha_s)$ were completed [4–6]. The diagrams involving a top quark are considered in [6] where the first five terms in the expansion for a heavy top quark mass, M_t, is computed. It was demonstrated that these terms approximate the exact result quite well. Actually it turned out that both at $\mathcal{O}(\alpha)$ and $\mathcal{O}(\alpha\alpha_s)$ a large cancellation between the sub-leading terms takes place and effectively only the leading term proportional to $G_F M_t^2$ [7] remains. This is a strong motivation to look at the next order in the strong coupling constant and evaluate the leading terms. To the corrections enhanced by the top quark mass only those contributions have to be considered where a scalar particle, namely the Higgs boson, H, the neutral Goldstone boson, χ, or the charged one, $\phi^\pm$, couples to the top quark. Thus no diagrams have to be considered where the W or Z boson appear as internal lines.

Corrections of this order were first computed for the ρ parameter [8], the ratio of the charged and neutral current amplitude, where it turned out that they are quite important [9]. Later on also the hadronic Higgs decay was analyzed at $\mathcal{O}(\alpha_s^2 G_F M_t^2)$ [10,11]. In the case of the Higgs boson one can exploit that the scalar coupling is proportional to the mass which simplifies the construction of an effective Lagrangian and especially the subsequent evaluation of the diagrams. Actually the whole computation could be reduced to the evaluation of two-point functions. We will see below that in the case of the Z boson one should also consider vertex diagrams.

It has become customary to parametrize the corrections proportional to M_t^2 by the quatity

$$X_t = \frac{G_F M_t^2}{8\pi^2\sqrt{2}}\,, \tag{1}$$

respectively the quantity x_t which is defined using the $\overline{\rm MS}$ definition of the top quark mass, m_t.

The quantum corrections to $\Gamma(Z \to b\bar{b})$ are divided into universal ones which are identical for all quark species and non-universal parts which are specific for the $Zb\bar{b}$ vertex. Both the universal and non-universal corrections are divided into singlet and non-singlet parts. The singlet contributions arise from those diagrams where the Z boson and the bottom quarks of the final state couple to different fermion lines. Another class of singlet contributions is constituted by the diagrams where the Z boson couples to two charged Goldstone bosons which in turn form together with two gluons a box diagram and the gluons finally couple to the quarks in the final state. In Fig. 1 some sample diagrams are listed. Figure 1a and b are of universal nature whereas in c the Goldstone boson in directly coupled to the final state bottom quark thus providing a non-universal contribution. In this article only non-singlet diagrams will

⋆ This work was supported by DFG under Contract Ku 502/8-1 and the *Schweizer Nationalfonds*

[a] *Permanent address:* Institute for Nuclear Research, Russian Academy of Sciences, 60th October Anniversary Prospect 7a, 117312 Moscow, Russia

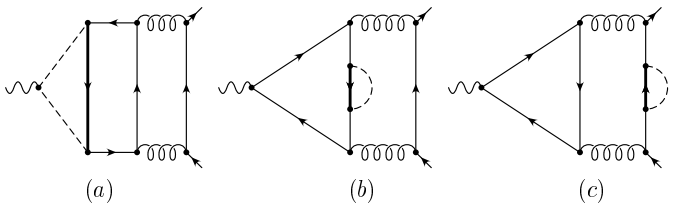

Fig. 1a–c. Singlet diagrams contributing at $\mathcal{O}(\alpha_s^2 X_t)$ to the hadronic Z boson decay. In **a** and **c** the dashed line correspond to the charged Goldstone boson whereas in **b** it may also be the Higgs or the neutral Goldstone boson. Diagrams **a** and **b** are of universal type whereas **c** constitutes a non-universal contribution to $\Gamma(Z \to b\bar{b})$. In the displayed examples the thick lines correspond to top quarks whereas the thin lines represent bottom quarks

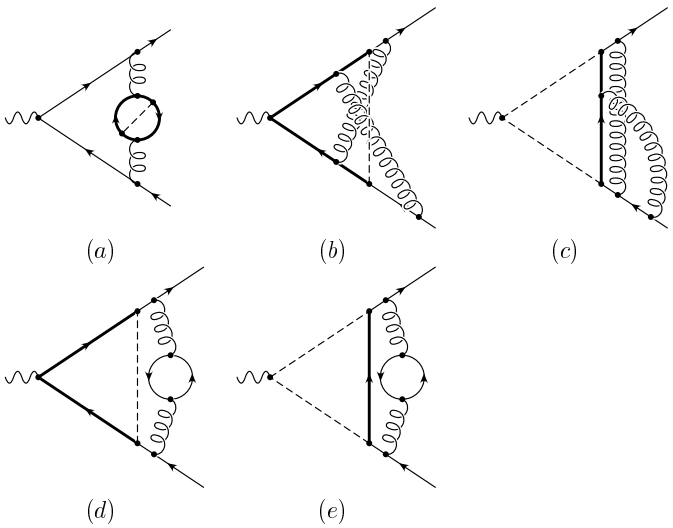

Fig. 2a–e. Non-singlet contributions of $\mathcal{O}(\alpha_s^2 X_t)$ to the hadronic Z boson decay. In **a** the dashed line corresponds to the Higgs boson or the neutral or charged Goldstone boson. In the diagrams **b**–**e** only the charged Goldstone boson is allowed. Diagram **a** is of universal type whereas **b**–**e** constitute non-universal contributions to $\Gamma(Z \to b\bar{b})$. In the displayed examples the thick lines correspond to top quarks whereas the thin lines represent bottom quarks

be computed; the singlet contributions will be considered elsewhere. The universal corrections of $\mathcal{O}(\alpha_s^2 X_t)$ are in part governed by the ρ parameter [9]. A second source for universal corrections arise from those diagrams where only gluons couple to the light quark lines. The gluons split into a fermion loop actually formed by bottom and top quarks accompanied by an additional exchange of a scalar particle (cf. Fig. 2a). The main focus of this paper is devoted to the evaluation of the non-universal non-singlet diagrams. Typical examples are pictured in Fig. 2b–e.

In a first step an effective Lagrangian is constructed were the top quark is integrated out. Thereby it is convenient to split the fermion fields into their left and right part and consider them separately. It is furthermore necessary to decouple the bottom quark fields using the relations (see e.g. [10]):

$$b_{L/R}^{0\prime} = \sqrt{\zeta_{2,b}^{0,L/R}}\, b_{L/R}^{0}\,, \tag{2}$$

where the primes denote the quantities in the effective theory and the superscript "0" reminds that we are still dealing with bare quantities. The decoupling constants $\zeta_{2,b}^{0,L/R}$ can be computed with the help of

$$\zeta_{2,b}^{0,L/R} = 1 + \Sigma_{b,V}^{0h} \mp \Sigma_{b,A}^{0h}\,, \tag{3}$$

where $\Sigma_{b,V}^{0h}$ and $\Sigma_{b,A}^{0h}$ is the vector and axial-vector part of the bottom quark self energy. Here only the hard part, i.e. those diagrams containing the top quark, has to be computed which is indicated by the index "h". Finally the part of the effective Lagrangian describing the interaction of the Z boson to bottom quarks has the form

$$\mathcal{L}_{\rm eff} \sim \left[C_L^0 \bar{b}_L^{0\prime}\gamma^\mu b_L^{0\prime} + C_R^0 \bar{b}_R^{0\prime}\gamma^\mu b_R^{0\prime}\right] Z_\mu\,. \tag{4}$$

The residual dependence on M_t is contained in the coefficient functions $C_{L/R}^0$. They are obtained from the hard part of the $Zb\bar{b}$ vertex:

$$C_{L/R}^0 = \frac{\Gamma_{Zb\bar{b}}^{h,L/R}}{\zeta_{2,b}^{0,L/R}}\,. \tag{5}$$

Here, the left and right part of the $Zb\bar{b}$ vertex are defined through:

$$\begin{aligned}\Gamma_{Zb\bar{b},\mu}^{h} &= \gamma_\mu\left[\Gamma_{Zb\bar{b}}^{h,V} + \gamma_5\Gamma_{Zb\bar{b}}^{h,A}\right]\,,\\ \Gamma_{Zb\bar{b}}^{h,L/R} &= \Gamma_{Zb\bar{b}}^{h,V} \mp \Gamma_{Zb\bar{b}}^{h,A}\,,\end{aligned} \tag{6}$$

where it is understood that in addition to the top-induced diagrams also the tree-level terms are included. The coefficient functions of (5) are finite after the coupling constant α_s and the mass of the top quark are expressed through their renormalized counterparts. This is because the vector and axial-vector currents have vanishing anomalous dimension as long as only non-singlet diagrams are considered. Thus from now on the index "0" is omitted.

In order to evaluate the partial decay rate of the Z boson into bottom quarks at $\mathcal{O}(\alpha_s^2 X_t)$ one has to evaluate the coefficient functions up to this accuracy. Furthermore the pure QCD corrections in the effective theory are needed up to order α_s^2. It can be taken over from [12] and reads:

$$\begin{aligned}&\delta^{(5),QCD}\\ &= 1 + \frac{\alpha_s^{(5)}(\mu)}{\pi} + \left(\frac{\alpha_s^{(5)}(\mu)}{\pi}\right)^2\left[\frac{365}{24} - 11\,\zeta_3\right.\\ &\quad\left. + n_l\left(-\frac{11}{12} + \frac{2}{3}\,\zeta_3\right) + \left(-\frac{11}{4} + \frac{1}{6}n_l\right)\ln\frac{M_Z^2}{\mu^2}\right],\end{aligned} \tag{7}$$

where $n_l = 5$ is the number of light quarks and ζ_i is Riemann's Zeta function with the value $\zeta_3 \approx 1.202056903$.

The computation of the decoupling constants for the bottom quark field up to order $\alpha_s^2 X_t$ has been performed

in [10]. The only missing pieces are the vector and axial-vector contributions to the hard part of the $Zb\bar{b}$ vertex. Some sample diagrams are listed in Fig. 2. As mentioned above only those diagrams have to be taken into account which contain a virtual top quark. Note that for the very calculation it is possible to nullify all external momenta. At one-loop order only two diagrams have to be considered. This increases to 19 at the two-loop level which is still feasible by hand. In the order we are interested in, however, more than 350 diagrams have to be considered, which makes the extensive use of computer algebra necessary. For the present calculation the package `GEFICOM` [13] has been used. It passes the generation of the diagrams to `QGRAF` [14] and uses for the very computation of the integrals the program `MATAD` [15] which is written in `FORM` [16] for the purpose to compute one-, two- and three-loop vacuum graphs. For a recent review concerned with the automatic computation of Feynman diagrams see [17].

Expressed in terms of the $\overline{\rm MS}$ top quark mass the result for the coefficient functions read:

$$
\begin{aligned}
C_L = \frac{e}{s_\theta c_\theta}\Bigg\{ &-\frac{1}{2}+\frac{1}{3}s_\theta^2 + x_t\Bigg[1+\frac{\alpha_s^{(6)}(\mu)}{\pi}C_F\left(2-\frac{3}{2}\zeta_2\right.\\
&\left.+\frac{3}{2}\ln\frac{\mu^2}{m_t^2}\right)+\left(\frac{\alpha_s^{(6)}(\mu)}{\pi}\right)^2\Bigg(C_F^2\Bigg(-\frac{49}{192}-\frac{199}{48}\zeta_2\\
&+\frac{253}{12}\zeta_3-\frac{77}{8}\zeta_4+\frac{5}{4}B_4-\frac{5}{8}D_3-\frac{1053}{32}S_2\\
&+\left(\frac{15}{16}-\frac{9}{4}\zeta_2\right)\ln\frac{\mu^2}{m_t^2}+\frac{9}{8}\ln^2\frac{\mu^2}{m_t^2}\Bigg)\\
&+C_AC_F\Bigg(\frac{461}{64}-\frac{99}{32}\zeta_2-\frac{187}{24}\zeta_3+\frac{61}{16}\zeta_4-\frac{5}{8}B_4\\
&+\frac{5}{16}D_3+\frac{1053}{64}S_2+\left(\frac{185}{48}-\frac{11}{8}\zeta_2\right)\ln\frac{\mu^2}{m_t^2}\\
&+\frac{11}{16}\ln^2\frac{\mu^2}{m_t^2}\Bigg)+C_FTn_l\Bigg(-\frac{95}{48}+\frac{4}{3}\zeta_2-\zeta_3\\
&+\left(-\frac{13}{12}+\frac{1}{2}\zeta_2\right)\ln\frac{\mu^2}{m_t^2}-\frac{1}{4}\ln^2\frac{\mu^2}{m_t^2}\Bigg)\\
&+C_FT\Bigg(\frac{149}{240}-\frac{1}{60}\zeta_2-\frac{35}{8}\zeta_3+\frac{729}{40}S_2\\
&+\left(-\frac{13}{12}+\frac{1}{2}\zeta_2\right)\ln\frac{\mu^2}{m_t^2}-\frac{1}{4}\ln^2\frac{\mu^2}{m_t^2}\Bigg)\Bigg)\Bigg]\Bigg\}\\
= \frac{e}{s_\theta c_\theta}\Bigg\{ &-\frac{1}{2}+\frac{1}{3}s_\theta^2 + x_t\Bigg[1+\frac{\alpha_s^{(6)}(\mu)}{\pi}\left(\frac{8}{3}-2\zeta_2\right.\\
&\left.+2\ln\frac{\mu^2}{m_t^2}\right)+\left(\frac{\alpha_s^{(6)}(\mu)}{\pi}\right)^2\Bigg(\frac{62149}{2160}-\frac{21337}{1080}\zeta_2\\
&+\frac{367}{108}\zeta_3-\frac{67}{36}\zeta_4-\frac{5}{18}B_4+\frac{5}{36}D_3+\frac{1557}{80}S_2\\
&+n_l\left(-\frac{95}{72}+\frac{8}{9}\zeta_2-\frac{2}{3}\zeta_3\right)+\Bigg(\frac{589}{36}-\frac{55}{6}\zeta_2\\
&+n_l\left(-\frac{13}{18}+\frac{1}{3}\zeta_2\right)\Bigg)\ln\frac{\mu^2}{m_t^2}\\
&+\left(\frac{55}{12}-\frac{1}{6}n_l\right)\ln^2\frac{\mu^2}{m_t^2}\Bigg)\Bigg]\Bigg\}, \qquad (8)\\
C_R = \frac{e}{s_\theta c_\theta}\frac{1}{3}s_\theta^2,&
\end{aligned}
$$

with $m_t = m_t(\mu)$. After the second equal sign the colour factors $C_F = 4/3, C_A = 3$ and $T = 1/2$ have been inserted. $\zeta_2 = \pi^2/6$ and $\zeta_4 = \pi^4/90$. s_θ and c_θ are the sine and cosine of the weak mixing angle. The constants B_4, D_3 and S_2 typically appear in the result of three-loop vacuum integrals and read [18,9,19]:

$$
\begin{aligned}
S_2 &= \frac{4}{9\sqrt{3}}\mathrm{Cl}_2\left(\frac{\pi}{3}\right) \approx 0.260\,434\,,\\
D_3 &= 6\zeta_3-\frac{15}{4}\zeta_4-6\left(\mathrm{Cl}_2\left(\frac{\pi}{3}\right)\right)^2 \approx -3.027\,009\,,\\
B_4 &= 16\mathrm{Li}_4\left(\frac{1}{2}\right)-\frac{13}{2}\zeta_4-4\zeta_2\ln^2 2\\
&\quad+\frac{2}{3}\ln^4 2 \approx -1.762\,800\,. \qquad (9)
\end{aligned}
$$

Note that according to the QED Ward identity the universal corrections induced by the diagrams in Fig. 2a cancel in the coefficient functions against the corresponding part in the quark self energy. As we consider in addition the bottom quark to be massless the right-handed coefficient function sticks to its Born value. Using the relation between m_t and the on-shell mass M_t [20] one gets:

$$
\begin{aligned}
C_L^{OS} = \frac{e}{s_\theta c_\theta}\Bigg\{ &-\frac{1}{2}+\frac{1}{3}s_\theta^2 + X_t\Bigg[1-2\zeta_2\frac{\alpha_s^{(6)}(\mu)}{\pi}\\
&+\left(\frac{\alpha_s^{(6)}(\mu)}{\pi}\right)^2\Bigg(\frac{1054}{135}-\frac{19897}{1080}\zeta_2+\frac{403}{108}\zeta_3\\
&-\frac{67}{36}\zeta_4-\frac{4}{3}\zeta_2\ln 2-\frac{5}{18}B_4+\frac{5}{36}D_3+\frac{1557}{80}S_2\\
&+n_l\left(-\frac{1}{3}+\frac{14}{9}\zeta_2-\frac{2}{3}\zeta_3\right)\\
&+\left(-\frac{31}{6}+\frac{1}{3}n_l\right)\zeta_2\ln\frac{\mu^2}{M_t^2}\Bigg)\Bigg]\Bigg\}, \qquad (10)\\
C_R^{OS} = C_R\,.&
\end{aligned}
$$

Let us now turn to a brief numerical discussion of the new results. The decay rate can be computed with the help of

$$
\Gamma(Z\to b\bar{b}) = \frac{N_C M_Z}{24\pi}\left(C_L^2+C_R^2\right)\delta^{(5),QCD}\,. \qquad (11)
$$

Actually two scales are involved in the process, namely M_Z and the mass of the top quark. The resummation of potentially large logarithms is, however, trivial as both $C_{L/R}$ and $\delta^{(5),QCD}$ are separately renormalization group invariant. Thus the scale parameter μ may be set to m_t, respectively, M_t in the coefficient functions and to M_Z in the massless corrections. For these choices the numerical

expansions of the ingredients for (11) read:

$$\delta^{(5),QCD} = 1 + \frac{\alpha_s^{(5)}(M_Z)}{\pi} + 1.409 \left(\frac{\alpha_s^{(5)}(M_Z)}{\pi}\right)^2,$$

$$C_L = \frac{e}{s_\theta c_\theta}\left\{ -\frac{1}{2} + \frac{1}{3}s_\theta^2 + x_t\left[1 - 0.623\frac{\alpha_s^{(6)}(\mu_t)}{\pi} + 0.190\left(\frac{\alpha_s^{(6)}(\mu_t)}{\pi}\right)^2\right]\right\},$$

$$C_L^{OS} = \frac{e}{s_\theta c_\theta}\left\{ -\frac{1}{2} + \frac{1}{3}s_\theta^2 + X_t\left[1 - 3.290\frac{\alpha_s^{(6)}(M_t)}{\pi} - 9.288\left(\frac{\alpha_s^{(6)}(M_t)}{\pi}\right)^2\right]\right\}, \quad (12)$$

with $\mu_t = m_t(m_t)$. $n_l = 5$ has been chosen.

Concerning the enhanced corrections of $\mathcal{O}(X_t)$ to the coefficient functions the same observations can be made as for the ρ parameter [9] and the various quantities in connection with the Higgs decay [21,10]: Expressed in terms of the on-shell top quark mass the leading order term is "screened" by the QCD corrections as they enter with a different sign. On the other hand, the coefficients turn out to be much smaller in the $\overline{\rm MS}$ scheme. Actually the coefficient in front of the three-loop term is smaller by a factor of 50 as compared to the corresponding one in the on-shell scheme. Furthermore the sign is alternating which also indicates a faster convergence if the $\overline{\rm MS}$ mass is used for the parameterization.

Inserting (12) into (11) finally leads to the following M_t^2-enhanced terms:

$$\Gamma^{x_t}(Z \to b\bar{b}) = \frac{N_C M_Z \alpha}{6 s_\theta^2 c_\theta^2}\left(-1 + \frac{2}{3}s_\theta^2\right) \times x_t\left[1 + 0.0161 + 0.0014\right], \quad (13)$$

$$\Gamma_{OS}^{X_t}(Z \to b\bar{b}) = \frac{N_C M_Z \alpha}{6 s_\theta^2 c_\theta^2}\left(-1 + \frac{2}{3}s_\theta^2\right) \times X_t\left[1 - 0.074 - 0.0130\right], \quad (14)$$

where the values $\alpha_s^{(5)}(M_Z) = 0.118$, $\alpha_s^{(6)}(M_t) = 0.107$ and $\alpha_s^{(6)}(m_t) = 0.108$ have been used. The numbers in the squared brackets correspond to the corrections with increasing power in α_s. The index OS reminds on the definition of the top quark mass used and as before the index $\overline{\rm MS}$ is suppressed. In the $\overline{\rm MS}$ scheme the second order QCD corrections amount to roughly 9% of the first order ones, however, the overall size is quite small. The order α_s corrections to the leading X_t term in the on-shell scheme is almost by a factor of five larger than in the $\overline{\rm MS}$ scheme and the corresponding $\mathcal{O}(\alpha_s^2)$ corrections amount to almost 18% of the $\mathcal{O}(\alpha_s)$ term. It is actually almost as large as the $\mathcal{O}(\alpha_s)$ term in (13).

To summarize, quantum corrections of $\mathcal{O}(\alpha_s^2 x_t)$ to the decay of the Z boson into bottom quarks have been computed. If we assume that the observations made at one- and two-loop level are also true at order $\alpha_s^2 X_t$ a substantial part of the corrections is available. Expressed in terms of the $\overline{\rm MS}$ mass they turn out to be tiny. In the on-shell scheme the quantum corrections are much larger and they screen the leading X_t term by almost 9%. Note that the newly computed term of $\mathcal{O}(\alpha_s^2 x_t)$ makes it possible to use the combination of the three-loop ρ parameter [9] and the partial width $\Gamma(Z \to b\bar{b})$ in a consistent way.

References

1. D. Karlen, talk presented at ICHEP '98, Vancouver, July 1998; W. Hollik, talk presented at ICHEP '98, Vancouver, July 1998; F. Teubert, Proceedings of the *IVth Int. Symp. on Radiative Corrections*, Barcelona, Sept. 8-12, 1998; hep-ph/9811414.
2. K.G. Chetyrkin, J.H. Kühn, and A. Kwiatkowski, *Phys. Reports* **277** (1996) 189.
3. A. Akhundov, D. Bardin, and T. Riemann, *Nucl. Phys.* **B 276** (1986) 1; W. Beenakker and W. Hollik, *Z. Phys.* **C 40** (1988) 141; J. Bernabeu, A. Pich, and A. Santamaria, *Phys. Lett.* **B 200** (1988) 569; B.W. Lynn and R.G. Stuart *Phys. Lett.* **B 252** (1990) 676.
4. A.L. Kataev, *Phys. Lett.* **B 287** (1992) 209.
5. A. Czarnecki and J.H. Kühn, *Phys. Rev. Lett.* **77** (1996) 3955; (E) *ibid.* **80**(1998) 893.
6. R. Harlander, T. Seidensticker, and M. Steinhauser, *Phys. Lett.* **B 426** (1998) 125.
7. J. Fleischer, F. Jegerlehner, P. Rączka, and O.V. Tarasov, *Phys. Lett.* **B 293** (1992) 437; G. Buchalla and A. Buras, *Nucl. Phys.* **B 398** (1993) 285; G. Degrassi, *Nucl. Phys.* **B 407** (1993) 271; K.G. Chetyrkin, A. Kwiatkowski, and M. Steinhauser, *Mod. Phys. Lett.* **A 8** (1993) 2785.
8. M. Veltman, *Nucl. Phys.* **B 123** (1977) 89.
9. L. Avdeev, J. Fleischer, S. Mikhailov, and O. Tarasov, *Phys. Lett.* **B 336** (1994) 560, (E) *ibid.* **B 349** (1995) 597; K.G. Chetyrkin, J.H. Kühn, and M. Steinhauser, *Phys. Lett.* **B 351** (1995) 331; *Phys. Rev. Lett.* **75** (1995) 3394.
10. K.G. Cheyrkin, B.A. Kniehl, and M. Steinhauser, *Nucl. Phys.* **B 490** (1997) 19; *Phys. Rev. Lett.* **78** (1997) 594.
11. M. Steinhauser, *Phys. Rev* **D 59** (1999) 054005.
12. K.G. Chetyrkin, A.L. Kataev, and F.V. Tkachov, *Phys. Lett.* **B 85** (1979) 277; M. Dine and J. Sapirstein, *Phys. Rev. Lett.* **43** (1979) 668; W. Celmaster and R.J. Gonsalves, *Phys. Rev. Lett.* **44** (1980) 560.
13. K.G. Chetyrkin and M. Steinhauser, unpublished.
14. P. Nogueira, *J. Comp. Phys.* **105** (1993) 279.
15. M. Steinhauser, Ph.D. thesis, Karlsruhe University (Shaker Verlag, Aachen, 1996).
16. J.A.M. Vermaseren, *Symbolic Manipulation with FORM*, (Computer Algebra Netherlands, Amsterdam, 1991).
17. R. Harlander and M. Steinhauser, Report Nos. BUTP-98/28, TTP98-41 and hep-ph/9812357, (Bern, Karlsruhe, 1998), Prog. Part. Nucl. Phys. **43** (1999) 239 (in press).
18. D.J. Broadhurst, *Z. Phys.* **C 54** (1992) 54.
19. D.J. Broadhurst, Eur. Phys. J. C **8** (1999) 311.
20. N. Gray, D.J. Broadhurst, W. Grafe, and K. Schilcher, *Z. Phys.* **C 48** (1990) 673.
21. B.A. Kniehl and M. Steinhauser, *Nucl. Phys.* **B 454** (1995) 485; *Phys. Lett.* **B 365** (1996) 297.